Statistical Study on Precipitable Water Content Variations Observed with Ground-Based Microwave Radiometers

Kazumasa AONASHI, Tetsuya IWABUCHI[1], Yoshinori SHOJI

Meteorological Research Institute, Tsukuba, Ibaraki, Japan

Ryu OHTANI

Geological Survey of Japan, National Institute of Advanced Industrial Science and Technology, Tsukuba, Ibaraki, Japan

and

Ryu-ich ICHIKAWA

Communication Research Laboratory, Kashima, Ibaraki, Japan

(Manuscript received 18 April 2003, in revised form 27 September 2003)

Abstract

GPS analysis requires statistical information on temporal variations of precipitable water vapor content (PWC), since temporal variability of PWC is assumed in the analyses. Spatial scales of PWC variations also are necessary for incorporation of the analyzed GPS data into numerical weather prediction systems.

The objective of the present study is to investigate temporal and spatial characteristics of the PWC variations in Japan. For this purpose, slant-path PWC was observed with ground-based microwave radiometers (MWRs) for the directions of GPS satellites in the eastern part of the Kanto Plain during several observation periods in 2000 and 2001. Three components, vertical PWC, horizontal gradient and higher-order inhomogeneity, were retrieved from the slant-path observation data. Deviations of vertical PWC from ten-day averages (hereafter referred to as vertical deviations) were then calculated in order to remove seasonal changes of this component. Simultaneous observation data at three MWR sites also were used for the rough estimation of horizontal scales of the three PWC components.

The results show:

1) The vertical deviations marked were about 20 times as large amplitudes as the other two components, while the variations due to the gradient had even smaller amplitudes than the inhomogeneity;

2) The vertical deviations had large spectral power against periods around 5–6 days and 8–9 days, while the gradient was dominated by diurnal variations; and,

3) It was roughly estimated that the vertical deviations (gradient) had the horizontal scales of several hundred (several ten) kilometers. The horizontal scale of the PWC inhomogeneity was considered to be less than 10 km.

Corresponding author: Kazumasa Aonashi, Mailing address: Meteorological Research Institute, 1-1 Nagamine Tsukuba Ibaraki, 305-0052, Japan. E-mail: Aonashi@mri-jma.go.jp

1 Present affiliation: UCAR, Boulder, Colorado, USA

The vertical deviations (the gradient) were considered to be closely related with large-scale meteorological disturbances (local-scale circulations) on the basis of the above temporal and spatial characteristics.

1. Introduction

Global Positioning System (GPS) analysis software retrieves slant-path wet delay induced by the atmospheric humidity (Bevis et al. 1992). As Tralli and Litchen (1990) pointed out, the retrieved wet delay can change largely, depending on the temporal variability of precipitable water vapor content (PWC) assumed in the analysis. Hence, accurate GPS analysis requires statistical information on PWC variations in the real atmosphere.

Many GPS analysis software packages use a gradient mapping function of MacMillian (1995) to decompose the slant-path wet delay into three components, vertical PWC, horizontal gradient, and higher-order inhomogeneity. These humidity-related data are attractive as the inputs into numerical weather prediction (NWP) systems. For the assimilation, however, it is necessary to know spatial scales of the three components (Maanen 1981).

Some studies have already examined temporal variability of the vertical PWC or gradient, using ground-based microwave radiometers (MWRs). For example, Güldner and Spänkuch (1999) employed yearly MWR data in central Europe for their statistical analysis.

However, little attention has been paid to the spatial scales of PWC variations. It is also expected that temporal PWC variations in central Europe are distinct from those in Japan that is located around the moisture-rich 'storm track' in the northwest Pacific. Accordingly, the objective of the present study is to investigate temporal and spatial characteristics of the PWC variations in the Kanto Plain, Japan.

For this purpose, we operated MWRs to observe slant-path PWC in the eastern part of the Kanto Plain over several periods in 2000 and 2001. We retrieved the three components of PWC from the observed data. We then analyzed amplitudes, temporal and horizontal characteristics of these PWC components.

2. Data used in the present study

2.1 Slant path PWC observation

In the present study, we operated dual-frequency MWRs (Radiometrics WVR1100) that automatically observed brightness temperatures (TBs) at 23.8 and 31.4 GHz along slant paths in the directions of all observable GPS satellites with time intervals of about 1 minute. The observation cycle usually took 10 to 12 minutes since about 10 GPS satellites were positioned above the horizon simultaneously.

Our MWR observations were performed in the following two manners:

1) To obtain long-term observation data, we operated a MWR at the Meteorological Research Institute (MRI) in Tsukuba (about 40 km north-east of Tokyo) for Aug. 3–Sep. 4, 2000, Sep. 27–Nov. 15, 2000, and Jan. 18–Feb. 13, 2001. (Hereafter these observation periods are referred to as OP1, 2, and 3.); and,

2) To estimate horizontal scales of PWC variations, we simultaneously operated MWRs at MRI, National Research Agricultural Center (NRAC, about 10 km west-southwest of MRI), and Communication Research Laboratory (CRL, about 50 km southeast of MRI) during Aug. 13–Sep. 2, 2001 (see Fig. 1). We chose this observation period (hereafter referred to as OP4) because we expected large spatial PWC differences in moisture-rich situations.

We retrieved slant-path PWC and liquid water content (LWC) from TBs by Radiometrics

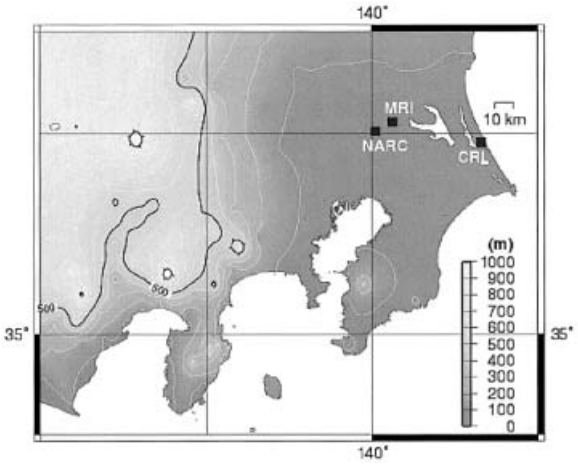

Fig. 1. Map of the MWR observation sites.

algorithm (Radiometrics Corp., 1998). To validate the retrieved PWC, we operated the MWRs at MRI, and compared the retrieved PWC with operational upper-air radiosonde observations in Tsukuba. The validation indicated that MWR PWC had high linear correlation with PWC derived from the radiosonde data. Though each MWR had different instrumental biases from the PWC derived using radiosonde observation data. Hence, we calibrated MWR PWC by the linear fitting method whose coefficients were determined based on the above comparison.

Then, using the threshold by Aonashi et al. (2000), we excluded possible rainy data with slant-path LWC over 0.5 sec θ kgm^{-2}, where θ denotes the elevation angle of the path. Low elevation angle data ($\theta < 30$ degrees) were also omitted because we found overestimation of MWR PWC for that elevation range, especially in moisture-rich situations. This overestimation was probably caused by a large field-of-view (about 5 degrees) of the MWR.

2.2 *Calculation of vertical, gradient, and inhomogeneity components of PWC*

Slant-path PWC at the elevation angle θ, and direction angle ϕ ($SPWC(\theta, \phi)$) can be divided into vertical PWC component ($PWCz$), variation due to PWC gradient ($Grd(\theta, \phi)$), and higher-order inhomogeneity (Inh):

$$SPWC(\theta, \phi)/m(\theta) = PWCz + Grd(\theta, \phi) + Inh, \quad (1)$$

where $m(\theta)$ is the mapping function that is approximated as sec θ in the present study. Using notation by MacMillan (1995), the variation due to PWC gradient is expressed as:

$$Grd(\theta, \phi) = \cot\theta(G_N \cos\phi + G_E \sin\phi), \quad (2)$$

where G_N (G_E) is the PWC gradient coefficient in north (east) direction.

We adopted the method by Aonashi et al. (2000) to retrieve hourly $PWCz, G_N$ and G_E from about 50 slant-path PWC observations for each hour, by minimizing the following cost function:

$$\sum_i \{SPWC(\theta_i, \phi_i)/m(\theta_i) - [PWCz + \cot\theta_i(G_N \cos\phi_i + G_E \sin\phi_i)]\}^2. \quad (3)$$

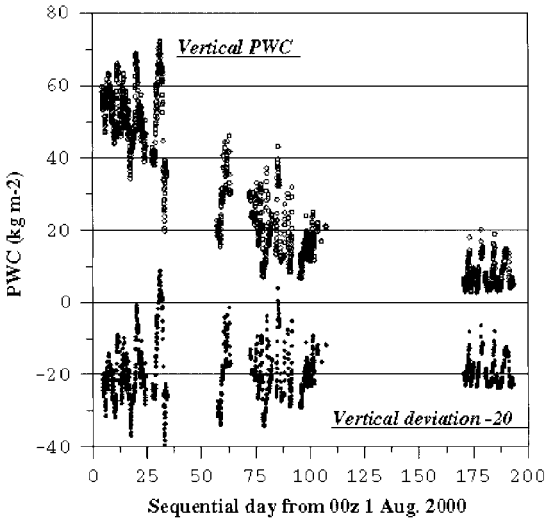

Fig. 2. Time sequence of the PWC variation at MRI for OP1–OP3 (units are kg m^{-2}). Circles and dots denote the vertical PWC and the vertical deviations minus 20 kg m^{-2}, respectively.

We then obtained the inhomogeneity component, Inh for each slant-path by substituting the above $PWCz, G_N$ and G_E into equation (1).

Figure 2 shows the time sequence of the vertical PWC for OP1–OP3. Besides variations with periods shorter than 10 days, the vertical PWC includes seasonal changes that are beyond the scope of the present study. We derived deviations from ten-day averages of the vertical PWC (hereafter referred as vertical deviations) to remove these changes. On the other hand, seasonal changes were not significant in the gradient and inhomogeneity (figure not shown).

3. Results

3.1 *Variation amplitudes of PWC*

Table 1 shows the averaged PWC and the standard deviations (STDs) of the vertical deviation, the variation due to the gradient, and the inhomogeneity component for OP1–OP3.

This table indicates that the vertical deviation marked about 20 times as large STDs as the other two components for the three periods, and that the observed PWC variations were dominated by the vertical deviation. On the other hand, the variation due to the gradient was even smaller than the inhomogeneity component. This suggests that the gradient map-

Table 1. Averaged PWC and STDs of the vertical deviation, the variation due to the gradient, and the inhomogeneity component for OP1–OP3 (units in kg m^{-2}).

	Averaged PWC	Vertical deviation ($PWCz$)	Variation due to the gradient ($Grd(\theta, \phi)$)	Inhomogeneity component (Inh)
OP1	44.012	8.888	0.252	0.346
OP2	15.395	6.102	0.203	0.273
OP3	4.538	3.498	0.130	0.242
OP1–OP3	25.280	7.014	0.232	0.325

ping function was not a good approximation, because of small amplitude of the PWC gradients in the Kanto Plain.

Comparing the variation amplitudes for the three periods, we also found that the STDs relative to the averaged PWC became larger as the season marched. For example, the vertical deviation had the STD comparable to the averaged PWC in winter (OP3), when large-scale extra-tropical lows were often developed along the 'storm track'.

3.2 Temporal scales of PWC variations

We estimated typical temporal scales of the 3 components for OP1–OP3, with spectral analysis of these data with respect to time. In this analysis, we adopted the Lomb algorithm (Press et al. 1992) to calculate spectral power from the observed data that included some periods without data.

Figure 3a plots the spectral power of the vertical deviation for OP1–OP3 against the period. This figure shows that variations with periods around 5–6 days, and 8–9 days were dominant in the vertical deviation. Comparing the spectral power during respective observation periods, we found small fluctuations in the predominant periods of the vertical deviation; OP2 had large spectral power for periods around 2–3 days (see Fig. 3b).

We also found that surface pressure in Tsukuba had similar temporal variations with the vertical deviation. For example, spectral power of the surface pressure for OP2 (Fig. 3c) agreed well with that of the vertical deviation (Fig. 3b).

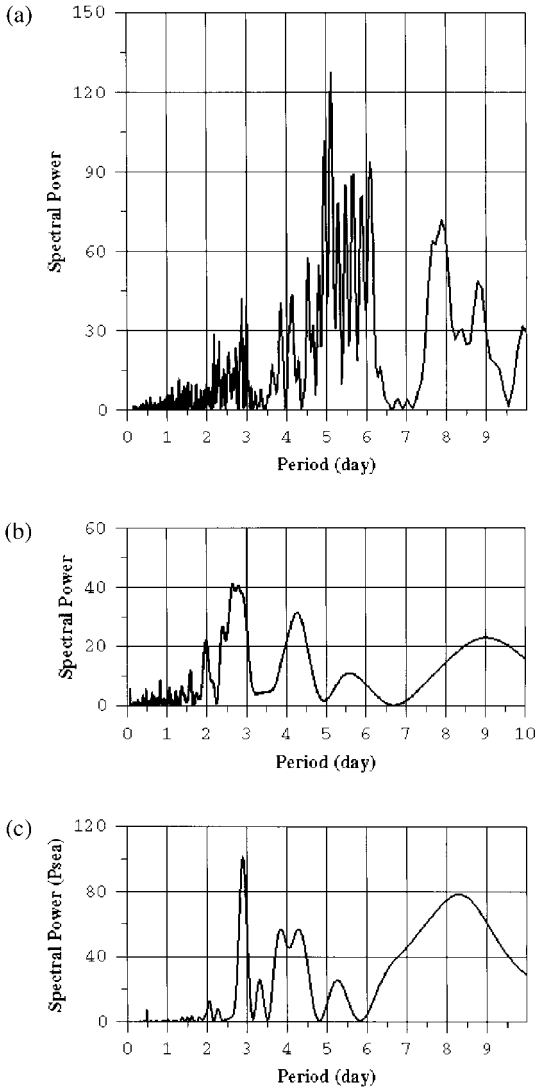

Fig. 3. Spectral power of (a) the vertical deviation for OP1–OP3 (unit is in 10^2 kg^2 m^{-4} sec^{-1}), (b) the vertical deviation for OP2 (unit is in 10^2 kg^2 m^{-4} sec^{-1}), (c) the surface pressure at MRI for OP2 (unit is in 10^6 Pa^2 sec^{-1}).

Since the surface pressure is the good index of large-scale extra-tropical low, we consider that the vertical deviation was also closely related to this disturbance.

Figure 4a (b) plots the spectral power of the variation due to the gradient (the inhomogeneity) for OP1–OP3. These figures show that the gradient was dominated diurnal variations while the inhomogeneity recorded large

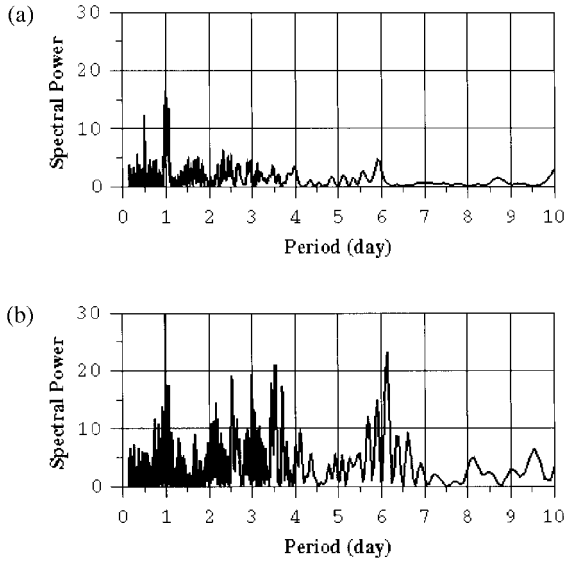

Fig. 4. Spectral power of (a) the variation due to the gradient, (b) the inhomogeneity component for OP1–OP3 (unit is in 10^2 kg^2 m^{-4} sec^{-1}).

spectral power for periods shorter than several days. It should be noted that near-daily peaks in the PWC gradient were also analyzed from slant-path MWR observations with a fixed elevation angle, which were performed by Aonashi et al. (2000). Accordingly, we consider that the diurnal variations in the gradient are the real atmospheric phenomena. (Although there is a possibility that observation in the GPS satellite directions can overestimate near-daily variations. (Elgered, personal communication))

3.3 Horizontal Scale of the PWC variations

Figure 5 displays scatter plots of the three components between MRI and NRAC for OP4. This indicates little spatial difference in the vertical deviation and large variability of the inhomogeneity on this horizontal scale (10 km).

To describe the horizontal scale of the PWC variations, we adopted Maanen's model (1981) that fits the correlation coefficient (*Corr*) of a

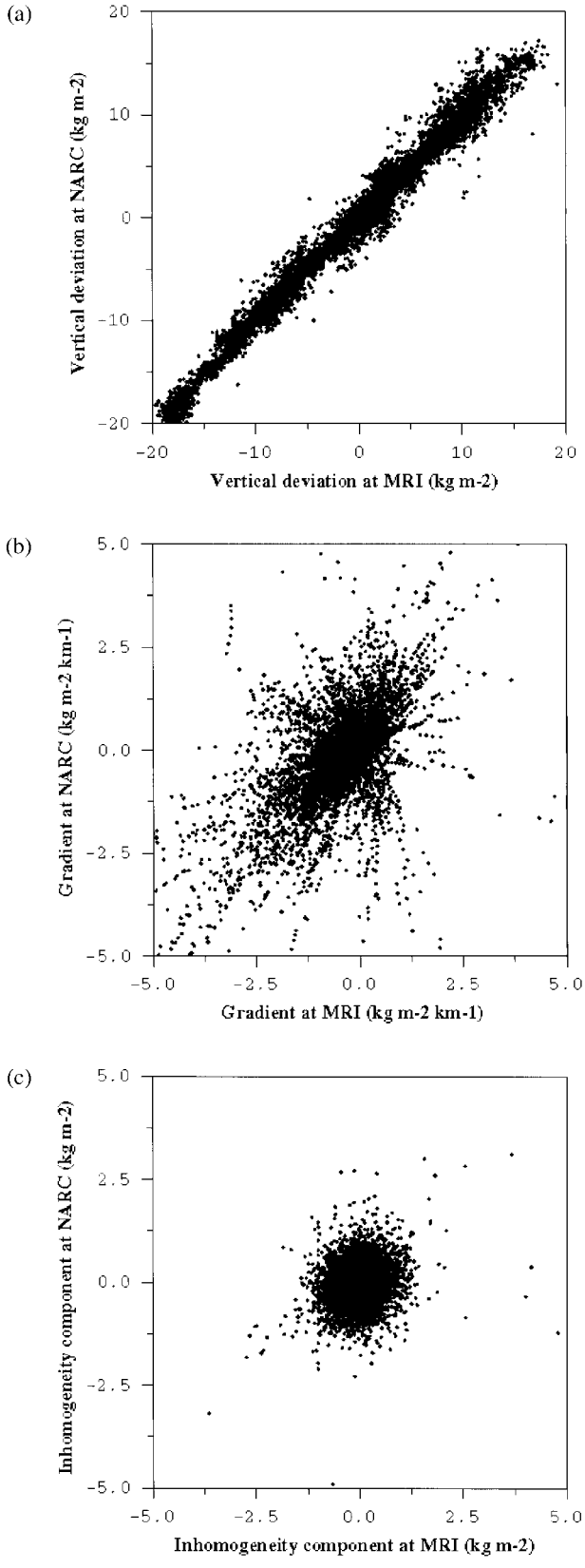

Fig. 5. Scatter plots of (a) the vertical deviation, (b) the gradient, (c) the inhomogeneity between MRI and NRAC for OP4.

Table 2. The correlation coefficients of the vertical deviation, the gradient and the inhomogeneity between the MWR sites for OP4.

	Vertical deviation	Gradient	Inhomogeneity
MRI-NRAC ($R \approx 10$ km)	0.986	0.420	0.176
MRI-CRL ($R \approx 50$ km)	0.912	0.227	0.120
NRAC-CRL ($R \approx 57$ km)	0.896	0.194	0.132

physical variable between different points in terms of the distance (R) as follows:

$$Corr = a \exp(-bR), \quad (4)$$

where a and b are fitting constants. The horizontal scale of the variable ($R0$) can be expressed as $1/b$.

Although we have only three MWR sites in the present study, we can roughly estimate the order of $R0$ by applying Maanen's model. For this purpose, we calculated correlation coefficients of the three components between the MWR sites for OP4 (Table 2).

The correlation of the vertical deviations was high (0.896), even between NRAC and CRL ($R \approx 57$ km). Thus, we considered that the horizontal scale of this component was on the order of several hundred kilometers, much larger than this distance. It should be noted that large-scale meteorological disturbances often have similar horizontal scales.

We then fitted the correlation coefficients of the gradient to equation (4). Based on the results, we estimated that the PWC gradient had the horizontal scale of several ten kilometers. This implies that the gradient was caused by local-scale circulations.

As shown in Table 2, correlation of the PWC inhomogeneity was negligible, even for the distance of 10 km. This means that the horizontal scale of the PWC inhomogeneity was considerably smaller than 10 km.

4. Summary and discussion

We made a statistical analysis to characterize the temporal and spatial PWC variations using the MWR observation data in the eastern part of the Kanto Plain over several observation periods in 2000 and 2001.

The results show:

1) The vertical deviation marked about 20 times as large amplitudes as the PWC variations due to the gradient and inhomogeneity. This means that the observed PWC variations were dominated by the vertical deviation;

2) The variation due to the gradient was even smaller than the inhomogeneity component;

3) The vertical deviation had large spectral power against periods around 5–6 days and 8–9 days, while the gradient was dominated by diurnal variations. The inhomogeneity recorded large spectral power against periods shorter than several days;

4) It is roughly estimated that horizontal scale of the vertical deviation (the gradient) was on the order of several hundred (several ten) kilometers. The horizontal scale of the PWC inhomogeneity was considered to be less than 10 km; and,

5) It is considered that the vertical deviation (variation due to the gradient) was closely related with large-scale extra-tropical low (local-scale circulation), on the basis of the above temporal and spatial characteristics.

The unique finding of the present study is the horizontal scales of the three components of the PWC variations. This result is expected to be applicable to assimilation of the GPS PWC data into NWP systems. We can also validate GPS analysis data by comparing this result with the horizontal scales of PWC variations derived from GPS data.

Comparing the above results with the study by Güldner and Spänkuch (1999), we found that the Kanto plain had larger vertical PWC variations than in central Europe, where the STD was 5 kg m^{-2} at most. Since the vertical PWC variation was closely related to large-scale extra-tropical lows, we consider that these large variations arose from development of the disturbances along the 'storm track' around Japan.

Another finding of the present study was that the PWC gradient was dominated by local-scale variations, (period of 1 day, horizontal scale of several ten kilometers). The result is consistent with Davis et al. (1993), in contrast to MacMillan and Ma (1997) that emphasized large-

scale variations in PWC gradients. On the basis of this result, we consider that GPS analysis should retrieve PWC gradients at least a few times a day for resolving local-scale variations.

Although the present study has revealed some statistical characteristics of PWC variability in the Kanto Plain, Japan, there still exist some problems:

1) At present, we do not have enough simultaneous observation sites to analyze horizontal scales of the PWC variation quantitatively;

2) PWC observation data are not available for rainy situations, where we expect the largest PWC variations; and,

3) We have not investigated PWC variations in mountainous regions where local-scale circulations are developed.

To address these problems, we will analyze PWC data obtained from dense GPS network observation campaigns in Tsukuba in 2000 and 2001. It is also necessary to study PWC variations in mountainous areas that occupy two thirds of Japan.

Acknowledgements

We express our thanks to Drs. Hajime Nakamura, Hiromu Seko and Masataka Murakami and Messrs. Ken-ichi Kusunoki and Takuya Kawabata for their kind cooperation and fruitful discussion, to Professors Tamio Takamura and Funitoshi Kimata for providing the microwave radiometers. The authors also thank the members of NRAC for their support for the observation. This work is a part of the GPS/MET Japan project financially supported by the Ministry of Education, Sports, Culture, Science and Technology of Japan.

References

Aonashi, K., Y. Shoji, R. Ichikawa, and H. Hanado, 2000: Estimating spatial variation of humidity from GPS and WVR observation in Tsukuba. *Earth, Planets and Space*, **52**, 907–912.

Bevis, M., S. Businger, T.A. Herring, C. Rocken, R.A. Anthes, and R.H. Ware, 1992: GPS Meteorology: Remote sensing of atmospheric water vapor using the Global Positioning System. *J. Geophys. Res.*, **97**, 15787–15801.

Davis, J.L., G. Elgered, A.E. Niell, and C.E. Kuehn, 1993: Ground-based measurement of gradients in the "wet" radio refractivity of air, *Radio Sci.*, **28**, 1003–1018.

Güldner, J. and D. Spänkuch, 1999: Results of year-round remotely sensed integrated water vapor by ground-based microwave radiometry. *J. Appl. Meteorol.*, **38**, 981–988.

Maanen, J.V., 1981: Objective analysis of humidity by the optimum interpolation method. *Tellus*, **33**, 113–122.

MacMillan, D.S., 1995: Atmospheric gradients from very long baseline interferometry observations. *Geophys. Res. Lett.*, **22**, 1041–1044.

——— and C. Ma, 1997: Atmospheric gradients and the VLBI terrestrial and celestial reference frame. *Geophys. Res. Lett.*, **24**, 453–456.

Press, W.H., S.A. Teukolsky, W.T. Vetterling, and B.P. Flannery, 1992: *Numerical Recipes in Fortran 77: The art of scientific computing, 2nd edition*, Cambridge university press, 933 pp.

Radiometrics Corp., 1998: *WVR 1100-water vapor and liquid water radiometer*, Radiometrics Corp., 32 pp.

Tralli, D.M. and S.M. Lichten, 1990: Stochastic estimation of tropospheric path delays in global positioning system geodetic measurements. *Bull. Geod.*, **64**, 127–159.